Reprint of paper CEAS / AIAA - 95 - 107 (1995)

THE SONIC BOOM OF AN OBLIQUE FLYING WING SST

Pei Li [1], Richard Seebass [2]

Aerospace Engineering Sciences

University of Colorado, Boulder

and

Helmut Sobieczky [3]

DLR German Aerospace Research Establishment

Göttingen, Germany

ABSTRACT

The oblique flying wing presents the real possibility of supersonic travel at fares not significantly greater than those for subsonic flight. One of its advantages is efficient operation at subsonic speeds. We provide general results for the sonic boom signature of an optimum oblique flying wing and give specific results for a nominal case, a 750 passenger transport flying at a Mach number of $\sqrt{2}$. Our results are general and may be used for any optimized oblique wing.

THE OBLIQUE FLYING WING (OFW)

Adolph Busemann was the first to point out, theoretically and experimentally, that wing sweep could be used to fly supersonically without the adverse wave drag of supersonic flight. [1, 2] R. T. Jones made the same discovery in the U.S. in 1944. [3, 4] Jones was flying hand launched oblique wing gliders as early as 1945. Busemann and Jones effectively considered a wing of infinite extent moving at a subsonic speed directly ahead. They then superimposed on this flow, a flow directly parallel to the wing's axis. If the speed of this flow along the wing is sufficiently large, then its vector addition to the flow normal to the leading edge will produce a supersonic flow obliquely toward the wing. Because the wing is infinite in extent, the flow over the wing behaves as if it were subsonic. This is true for an inviscid or a viscous flow. [4] One way to understand this, for inviscid flow at least, is to note that the shock wave emanating from the leading tip of a finite wing moves to infinity as the wing becomes infinite in extent.

If we could fly wings of infinite extent, we could fly supersonically without the penalty of wave drag provided the Mach number of the flow normal to the wing is subcritical. Higher normal Mach numbers are possible with a shock-free airfoil. Indeed, even if a shock wave occurs terminating a supersonic region of flow on the wing, the wave drag will be minimal because of the limited extent of the shock wave above the wing. This shock will thicken the boundary layer and the lift-to-drag ratio will decrease through the loss of lift caused by the decrease in circulation transported off the trailing edge of the wing. [5]

We cannot fly wings of infinite extent. Jones [6] was the first to point out that for a finite wing an oblique wing with an elliptical load distribution minimizes the wave and induced drag due to lift. Later, Smith [7] considered the optimum volume distribution for such wings. Lee [8] proposed a Mach 2 elliptic wing transatlantic transport. Sir Frederick Handley Page proposed just such an aircraft design for what eventually became the Concorde. [9] In his proposal the pilots sat in a small fuselage located on the leading tip of the oblique wing. The vertical tail was located on the trailing tip.

The reduction in the wave drag of an oblique wing of finite span comes from the very considerable length in the spanwise direction over which lift and volume are attained. Thus there is a clear advantage for the oblique wing over the swept wing. It was pointed out, humorously at the time we are told, that the oblique wing was the perfect compromise between the advocates of forward sweep and those of rearward sweep. The advantage of an oblique wing over a swept back (or forward) wing of comparable lift is clearly evident in the general expression for drag:

$$Drag = qS_f C_f + \frac{L^2}{\pi q b^2} + \frac{128 q V^2}{\pi l_v^4} + \frac{\beta^2 L^2}{2\pi q l_l^2} \cdot \qquad (1)$$

Here q is the dynamic pressure, S_f the reference area for skin friction, C_f the skin friction coefficient, L the lift, b

[1] Research Associate
[2] Professor
[3] Senior Research Scientist

the wing's span, V the wing's volume, and $\beta^2 = M^2 - 1$. The first two terms represent the drag due to skin friction and that induced by the trailing vortex sheet. The last two terms represent the wave drag due to volume and due to lift. The lengths in these two terms, l_v and l_l, are the average over all azimuthal angles of the effective length for volume and lift for each azimuthal angle.

We can see more clearly the advantages of wing sweep. Figures 1 and 2, taken directly from Jones [10, 11] make the point. The first compares the wave drag due to lift of an oblique and a swept wing for a given lift; the second compares the wave drag due to volume of an oblique wing and a swept wing as a function of the Mach number. We can escape the wave drag due to volume by paying a significant penalty in skin friction drag. The wave drag due to lift is inescapable, as is the sonic boom due to lift. [12, 13, 14]

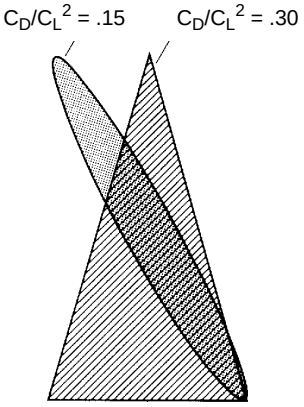

FIGURE 1. Drag due to lift. Oblique elliptic wing and delta wing, M = 1.4 (from Ref. 11 with publisher's permission).

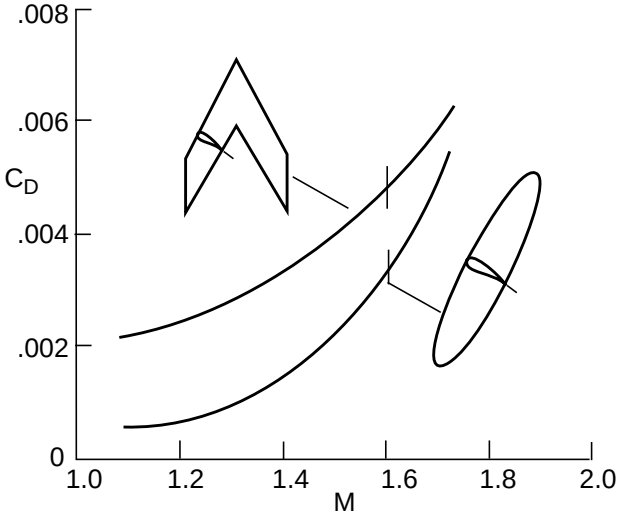

FIGURE 2. Wave drag due to volume of oblique elliptic and swept wings as a function of Mach number (Ref. 11).

AN OPTIMUM OBLIQUE FLYING WING

An oblique flying wing with the optimum load and thickness distributions provides the linear theory minimum for induced drag, wave drag due to lift, and wave drag due to volume. For an oblique flying wing, where the lifting element also provides the payload volume, the wave drag due to volume is inescapable. In addition, there is no distinction between the length over which the volume is distributed and the length over which the lift is generated. Consequently, for our studies, a single length, l, suffices. This length varies with the aspect angle θ from which the wing is viewed so we write $l(\theta)$. (See Figure 3.) It of course also depends on the wing sweep angle, λ, and the Mach angle, μ.

Studies by McDonnell Douglas Aerospace West [15, 16] provide good guidance on how many passengers a realistic OFW might carry, how much it might weigh, and at what speeds and altitudes it might fly for the Mach number range 1.3-1.6. These studies derive from and advance earlier work by Kroo, [17] Van der Velden, [18] Galloway, [19] and Waters. [20] Our own studies of supercritical airfoil design indicate that a 17% thick airfoil section can provide shock-free flow, if properly designed, up to a (normal) Mach number of 0.71 and perhaps higher. Swept to 60 degrees this implies a flight Mach number of about 1.42, or for that matter the square root of 2.

We choose a freestream Mach number of $\sqrt{2}$ for simplicity and a sweep angle of 60 degrees for ease of control and aeroelastic stability. Higher speeds are possible with more sweep, but the wing's control becomes increasingly difficult, with 60 degrees being judged acceptable in previous studies. [21, 22, 23, 24] In a recent Ph.D. dissertation, Morris [25] gives some evidence that this is a reasonable assumption on our part.

We use this recent McDonnell Douglas [15] study as a guide to conclude that a 750 passenger aircraft with a 5200 nautical mile (8368 kilometers) range will have a wing with a maximum chord of about 55 feet (16.8 meters) and a span, b, of about 475 feet (145 meters). This provides an aspect ratio of 11 and a wing area of 20,518 square feet (1906 square meters). These studies indicate this aircraft should have a direct operating cost of less than 6.5 cents per seat mile. Such an OFW transport might weigh 1.7 million pounds (771 metric tons) at takeoff, and reach a Mach number in excess of 1.15 with a weight of over 1.6 million pounds (726 metric tons). At this speed the sonic boom will first reach the ground and it will do so as a superboom. The theoretical and experimental magnitudes of these superbooms have been examined and at least satisfactory approximate results are available. [26, 27, 28, 29] We should also note that the upward propagating waves and

the waves reflected off the ground or ocean are refracted in the upper atmosphere where the sound speed increases nearly linearly with altitude and these provide a weak secondary acoustic signal at the ground associated with the aircraft's supersonic flight. [30, 31]

This OFW transport will enter cruise at about 1.575 million pounds (714 metric tons) and leave cruise at a weight of 0.905 million pounds (411 metric tons). While the volume of this wing is fixed its lift will vary considerably. Thus it is important to determine the OFW's sonic boom as a function of weight and volume. For our nominal conditions we take the weight to be 1.2 million pounds (544 metric tons), the volume to be 85,800 cubic feet (2430 cubic meters) and the altitude to be 42,000 feet (12.8 kilometers).

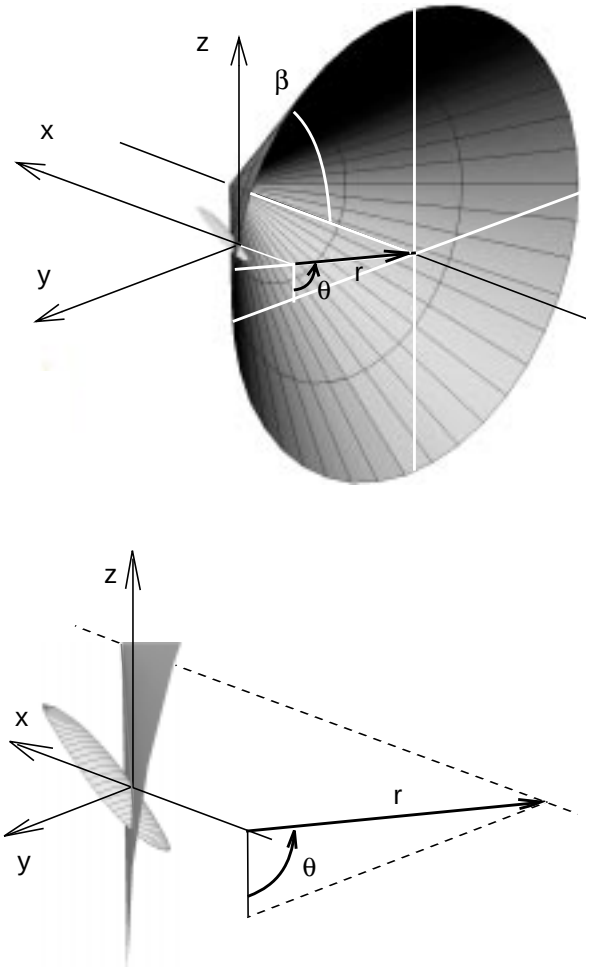

FIGURE 3. Fore-Mach cone (above) for the linearized solution, intersecting the OFW: detail below.

LINEAR FARFIELD OF THE OPTIMUM OFW

As noted above, we know the volume and the lift distribution of the optimum OFW. With these known, we can determine the linear farfield of this OFW for a homogeneous atmosphere. This we do following Lomax [32] who showed that the linear farfield in a given azimuthal plane, θ = const., as shown in Figure 3, is given by the Riemann-Liouville integral of order 1/2 of the second derivative of the area of an equivalent body of revolution. To do so Lomax used the wave equation analog of the Green's function for Laplace's equation, the Riemann function. [33] The linear pressure coefficient c_p at x-βr, θ, and with (x-βr)/r small, is simply the transform of the second derivative of the cross-sectional area of an equivalent body of revolution:

$$\pi l^{3/2}\sqrt{2\beta r}\,c_p(\chi;\theta) = \int_0^{\chi} \frac{[S''_l(\xi;\theta) + S''_v(\xi;\theta)]}{\sqrt{\chi-\xi}}\,d\xi \quad , \tag{2}$$

where $\chi = (x\text{-}\beta r)/l$ where $l(\theta)$ is the length of the equivalent body of revolution for the θ = const. azimuthal plane and $\xi = x/l$ the nondimensional coordinate in the x direction. The areas S retain their dimension of l^2 here, but their differentiation is with respect to the nondimensional variable $\xi = x/l$.

Here the area $S_l(\xi;\theta)$ is the area of the equivalent body of revolution due to lift given by

$$S_l(\xi;\theta) = \frac{\beta}{2q}\int_0^{\xi} \Lambda(t;\theta)\,dt \quad , \qquad 0 \le \xi \le 1, \tag{3}$$

where Λ is the component of force on the contour cut by the tangent to the fore-Mach cone emanating from the point x-βr, θ lying in a θ = const. plane and normal to the freestream. For the optimum OFW this area distribution must be the Karman ogive [34] area distribution that minimizes the wave drag associated with a given base area and

length:

$$S_l(\xi;\theta) = \frac{\beta L\cos\theta}{2\pi q}\times \qquad (4)$$
$$[\pi - \text{acos}(2\xi-1) + 2(2\xi-1)\sqrt{\xi(1-\xi)}],$$

The base area of this ogive is $\beta L\cos\theta/(2q)$.

The second term, $S_v(\xi;\theta)$, represents the area of the wing cut by the tangent to the fore-Mach cone emanating from the point x-βr and θ projected on to the local x = const. plane. For the optimum OFW this is the Sears [35]-Haack [36] area distribution for the given volume V and achieved over the length $l(\theta)$:

$$S_v(\xi;\theta) = \frac{128V}{3\pi l}[\xi(1-\xi)]^{3/2},$$
$$0\le\xi\le 1. \qquad (5)$$

The length in Equations (2)-(5) varies with θ and with the Mach angle μ according to

$$l = b[\sin\lambda - \beta\cos\lambda\sin\theta]. \qquad (6)$$

The lengths are a maximum on the side with the leading tip where $\theta = -\pi/2$ and a minimum on the side of the trailing tip where $\theta = \pi/2$. This leads to an asymmetry in the signal on the ground plane resulting in a maximum sonic boom overpressure and impulse at a positive θ. The values of these θs depend on the relative size of L and V.

For the nominal configuration considered here we give the results for the overpressure and impulse at $\theta = 0$ as well as their variation with θ. It is not known which of these is the principal contributor to sonic boom annoyance. [37, 38, 39] It is the authors' opinion that they are about equally important (see e.g. Ref. 9).

We should observe here that Van der Velden and Kroo, [40] in a paper on this same subject that was brought to our attention as we completed this manuscript, provide results for the pressure signature on the ground track and at $\theta = \pm 40^o$. While they note the maximum overpressure is offset from the ground track they do not give the maximum overpressure or the maximum impulse. Their approach is different from ours, however. They also provide no result for the impulse, an important parameter for sonic boom damage and indoor annoyance, nor for the variation of the overpressure and impulse with θ.

The general result for the linear pressure coefficient, with the lift, L, replaced by the aircraft's weight, W, is:

$$\pi\sqrt{2\beta\frac{r}{l}}c_p(\chi;\theta) \equiv \Im(\chi;\theta) = \qquad (7)$$
$$F_l(\chi;\theta) + F_v(\chi;\theta)\cdot$$

Here the dependence on θ is contained in the dependence of the two coefficients, A and B, on $l(\theta)$, where the contribution due to lift and that due to volume are respectively

$$F_l(\chi) = A(\theta)[F_1(\chi) - 2F_2(\chi)],$$

$$F_v(\chi) = B(\theta)[F_1(\chi) - 8F_3(\chi)],$$

with $A(\theta) = 2\beta W\cos\theta/(\pi q l^2)$, $B(\theta) = 32V/(\pi l^3)$, and the $F_i(\chi)$ are given by

$$F_1(\chi) = \int_0^\chi \frac{d\xi}{\sqrt{\xi(1-\xi)(\chi-\xi)}},$$

$$F_2(\chi) = \int_0^\chi \frac{\xi d\xi}{\sqrt{\xi(1-\xi)(\chi-\xi)}},$$

$$F_3(\chi) = \int_0^\chi \frac{\sqrt{\xi(1-\xi)}}{\sqrt{\chi-\xi}}d\xi \quad .$$

For $\chi \geq 1$ the upper limit of each integral is one. These functions are numerically integrated by representing the S_l'' and S_v'' distributions as a series of pulses as described in Ref. 41. The resulting functions $F_l(\chi;0)$ and $F_v(\chi;0)$ are shown in Figure 4.

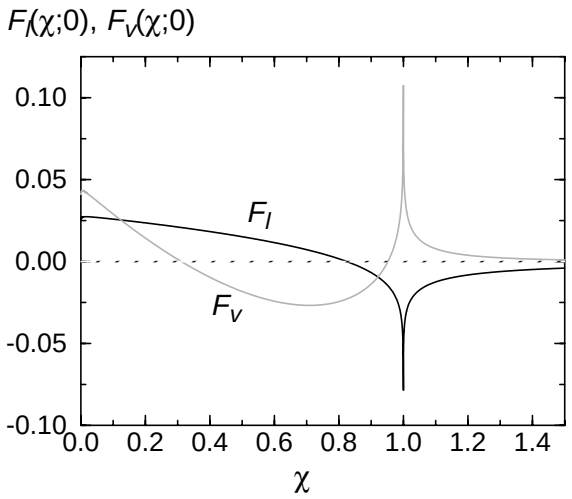

FIGURE 4. The functions $F_l(\chi;0)$ and $F_v(\chi;0)$ for $\theta = 0$.

SONIC BOOM OF THE OPTIMUM OFW

As noted earlier, we choose for nominal conditions an aircraft weighing 1.2 million pounds (544 metric tons) and flying at an altitude of 42,000 feet (12.8 kilometers). The wing section we have designed for this wing has a cross-sectional area of 354 square feet (32.9 square meters), which, with $Smax = 16V/(3\pi b)$, gives a volume of 99,830 cubic feet (2827 cubic meters). We assume, for simplicity, an isothermal atmosphere with a 25,000 foot (7.6 kilometer) scale height (density e-folding altitude). This approximation has been shown to be a very reasonable one. We also neglect winds.

The linear farfield pressure of the optimum OFW is determined for each azimuthal plane by

$$\pi\sqrt{2\beta\frac{r}{l}}c_p(\chi;\theta) = \Im(\chi;\theta)\cdot$$

For the nominal case given above this leads to the $\Im(\chi;0)$, depicted in Figure 5 for the $\theta = 0$ plane.

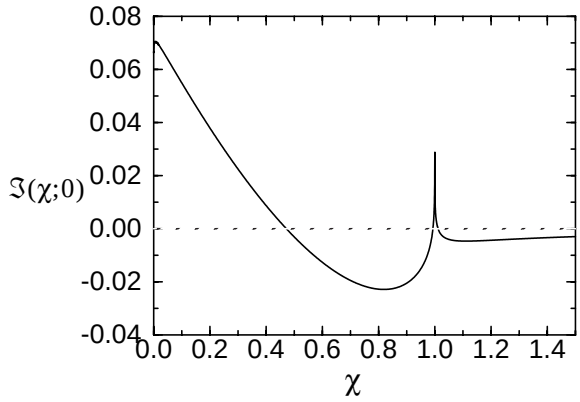

FIGURE 5. The function $\Im(\chi;0)$ for the nominal conditions given and $\theta = 0$.

We now need to correct this pressure signature for nonlinear and atmospheric effects. The effects of nonlinearity were first considered by Whitham [42] for bodies of revolution. The effects of the atmosphere can be treated simultaneously with nonlinearity. [12, 20] Rayleigh and Stokes understood well acoustic propagation in the atmosphere and Stokes considered the effects of winds in 1858. In the absence of winds the Rayleigh acoustic energy is conserved. With winds the Blokhintsev acoustic energy is conserved. [43]

The Rayleigh acoustic energy is $p'^2A/(\rho a)$, where p' is the pressure perturbation, A is the ray tube area and ρa, the product of the density and sound speed, is the acoustic impedance. For an isothermal atmosphere the ray tube area variation is already taken care of by the $\sqrt{r}$ multiplying c_p. The acoustic impedance increases as $exp(-z/H)$ where $-z$ is the distance below the aircraft. The pressure amplitudes need to be corrected by this factor to account for the change in acoustic impedance.

One effect remains to be accounted for: the nonlinear distortion of the signal. This is given by the advance, α, of one portion of the signal relative to the zero point of the signal because of its amplitude, which means its own velocity added to its effect on the local sound speed. Below the aircraft the maximum advance achieved in an isothermal atmosphere with exponentially increasing acoustic impedance is the same as that at a distance of $(\pi/2)H$ in a homogeneous atmosphere. [12] This nonlinear distortion makes the pressure multi-valued. The weak shock conditions lead to the conclusion that the multi-valued result is to be made single-valued by preserving its area.

The horizontal asymptotic nonlinear advance of the signal is given by, under the approximation of an isothermal atmosphere, [44]

$$\alpha = \frac{\Gamma M^4}{2\beta^{3/2}} \Im(\chi;\theta) \sqrt{\frac{Hl}{\pi \cos\theta}} erf \sqrt{\frac{r\cos\theta}{2H}}, \quad (8)$$

where $\Gamma = (\gamma + 1) / 2$ for a perfect gas.

Applying this advance to the signature in Figure 5, doubling the pressure for ground reflection and rendering the pressure single-valued with the appropriate addition of shock waves, one finds the pressure signature at the ground depicted in Figure 6.

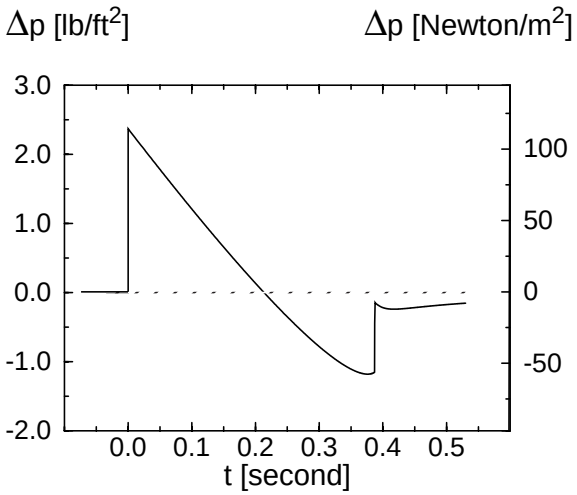

FIGURE 6. Pressure signature on the ground directly below the nominal OFW.

The ground trace given in Figure 6 provides an overpressure of 2.37 lb/ft^2 (113.5 Newton/m^2) and an integrated pressure loading over the positive phase, or impulse, of 0.25 lb-sec/ft^2 (11.8 Newton-sec/m^2). As we noted earlier, these will vary with θ because the length over which the pressure signature is generated (Equation (6)) and the lift contribution, vary with θ. An observer at π/2, for example, sees a length of $b[\sin\lambda - \beta\cos\lambda]$ or $0.366b$ for our nominal case, while an observer at $-\pi/2$ sees a length of $b[\sin\lambda + \beta\cos\lambda]$ or $1.366b$ for our nominal case. The overpressure and impulse thus vary laterally as depicted in Figures 7 and 8.

The principal effect of the variation of the sound speed with altitude, which we have neglected heretofore, is to refract the pressure signals beyond a limiting θ back into the troposphere leading to a lateral "cutoff" of the pressure signal felt on the ground. For our nominal conditions this corresponds to a θ of 63.5 degrees or a lateral distance of 84,200 feet (25.7 kilometers). This same effect alters somewhat the location of the pressures from those depicted in Figures 7 and 8.

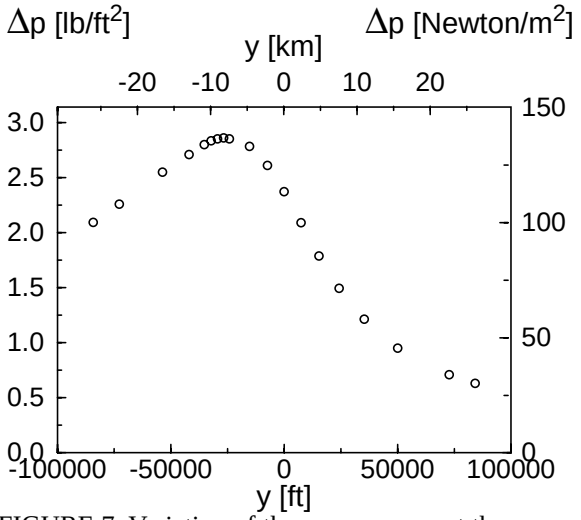

FIGURE 7. Variation of the overpressure at the ground with lateral distance.

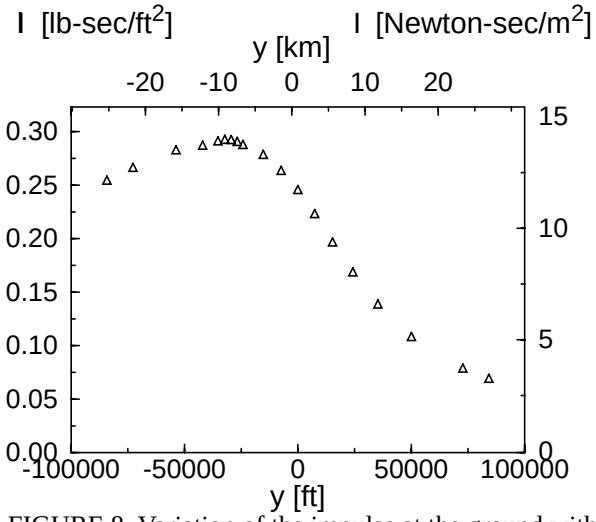

FIGURE 8. Variation of the impulse at the ground with lateral distance.

We conclude, then, that the nominal OFW considered here has a maximum shock pressure rise of 2.86 lb/ft^2 (136.8 Newton/m^2) and a maximum impulse of 0.293 lb-sec/ft^2 (14.02 Newton-sec/m^2). These occur at y = -

26,757 and -32,228 feet respectively (-8.16 and -9.82 kilometers). These are most unlikely to be acceptable. We note that the impulse is the principal contributor to indoor annoyance and structural damage. These results should not be surprising given that the shock pressure rise increases as the square root of the weight and only decreases as the quarter power of the length. [12, 44] The OFW is a long aircraft, but with 750 passengers, it is also a heavy aircraft.

CONCLUSION

The OFW has many features to commend it. They include low drag at all speeds, low structural weight, low airport noise, a fuel economy approaching that of subsonic jets, and the ability to carry a large number of passengers. And it can fly efficiently subsonically and efficiently at Mach numbers of 0.9-1.1 where there is no sonic boom on the ground. In supersonic flight over populated areas its sonic boom would not be acceptable.

Acknowledgement:

This work is funded by the German Alexander-Von-Humboldt Foundation through a 1991 Max Planck Research Award.

REFERENCES

1. Busemann, A., "Aerodynamischer Auftrieb bei Überschallgeschwindigkeit", *Proc. Volta Congress*, pp. 328-360, 1935.

2. Busemann, A., "Pfeilflügel bei Hochgeschwindigkeit", *Lilienthal-Gesellschaft*, Bericht 164, 1943.

3. Jones, R.T., "Wing Plan Forms for High-Speed Flight", *NACA TN* 863, 1947.

4. Jones, R.T., "Effects of Sweepback on Boundary Layer Separation", *NACA Rep.* 884, 1947.

5. Sobieczky, H. and Seebass, A.R., "Supercritical Airfoil and Wing Design", *Annual Reviews of Fluid Mechanics*, Vol. 16, pp. 337-363, 1984

6. Jones, R.T., "Theoretical Determination of the Minimum Drag of Airfoils at Supersonic Speeds", *J. Aero. Sci.*, Vol. 19, No. 12, pp. 813-822, 1952.

7. Smith, J.H.B., "Lift/Drag Ratios of Optimized Slewed Elliptic Wings at Supersonic Speeds", *Aeronautical Quart.*, Vol. 12, pp. 201-218, 1961.

8. Lee, G.H., "Comments on paper by D. Küchemann: 'Aircraft Shapes and their Aerodynamics'," *Advances in Aero. Sci.*, Vol. 3, pp. 250-252, 1962.

9. Wilson, A., *The Concorde Fiasco*, Penguin, p. 21, 1973.

10. Jones, R.T., *Wing Theory*, Princeton University Press, 1990.

11. Jones, R.T., "The Flying Wing Supersonic Transport", *Aero. J.*, Vol. 95, No. 943, pp. 103-106, March 1991.

12. Seebass, R., "Sonic Boom Theory", *J. Aircraft*, Vol. 6, No. 3, pp. 177-184, 1969.

13. Busemann, A., "The Relationship between Minimizing Drag and Noise at Supersonic Speeds", *High-Speed Aeronautics*, Polytechnic Institute of Brooklyn, pp. 133-144, 1955.

14. Seebass, A.R. and George, A.R., "Design and Operation of Aircraft to Minimize their Sonic Boom", *J. Aircraft*, Vol. 11, No. 9, pp. 509-517, 1974.

15. Rawdon, B.K., Scott, P.W., Liebeck, R.H., Page, M.A., Bird, R.S. and Wechsler, J., "Oblique All-Wing SST Concept", McDonnell Douglas Contractor Report, NAS1-19345, 1994. (Also private communication from B. Rawdon.)

16. Agrawal, S., Liebeck, R.H., Page, M.A. and Rodriguez, D.L., "Oblique All-Wing Configuration: Aerodynamics, Stability and Control", McDonnell Douglas Corporation Final Report, NAS1-19345, 1993.

17. Kroo, I., "The Aerodynamic Design of Oblique Wing Aircraft", AIAA Paper 86-2624, 1986.

18. Van der Velden, A., "Aerodynamic Design and Synthesis of the Oblique Flying Wing Supersonic Transport", Ph.D. Dissertation, SUDDAR 621, Stanford University, May 1992.

19. Galloway, T., Gelhausen, P., Moore, M. and Waters, M., "Oblique Wing Supersonic Transport", AIAA Paper 92-4230, 1992.

20. Waters, M.H., Ardema, M.D., Roberts, C. and Kroo, I., "Structural and Aerodynamic Considerations for an Oblique All-Wing Aircraft", AIAA Paper 92-4220, 1992.

21. Campbell, J.P. and Drake, H.M., "Investigation of Stability and Control Characteristics of an Airplane Model with a Skewed Wing in the Langley Free Flight Tunnel", *NACA TN* 1208, May 1947.

22. Curry, R.E. and Sim, A.G., "Unique Flight Characteristics of the AD-1 Oblique-Wing Research Airplane", *J. Aircraft*, Vol. 20, No. 6, pp. 564-568, 1983.

23. Kempel, R., McNeill, W., Gilyard, G. and Mane, T.,

"A Piloted Evaluation of an Oblique Wing Research Aircraft Motion Simulation with Decoupling Control Laws", *NASA TP* 2874, Nov. 1988.

24. Jones, R.T. and Nisbet, J.W., "Aeroelastic Stability and Control of an Oblique Wing", *Aero. J.*, pp. 365-369, August 1976.

25. Morris, S., "Integrated Aerodynamic and Control System Design of Oblique Wing Aircraft", Ph.D. Dissertation, Stanford University, January 1990.

26. Gill, P.M. and Seebass, R., "Nonlinear Acoustic Behaviour at a Caustic", *Prog. Astro. and Aero.*, Vol. 38, pp. 353-386, 1975.

27. Cramer, M.S. and Seebass, A.R., " Focusing of Weak Shock Waves at an Arete", *J. Fluid Mech.*, Part 2, Vol. 88, pp. 209-222, 1978.

28. Fung, K.Y., "Shock Wave Formation at a Caustic", *SIAM J. Appl. Math.*, Vol. 39, No. 2, pp. 355-371, 1980.

29. Wanner, J.-C., Vallee, J., Vivier, C. and Thery, C., "Theoretical and Experimental Studies of the Focus of Sonic Boom", *J. Acoust. Soc. Am.*, Vol. 52, No. 1 (Part 1), pp. 13-32, 1972.

30. Rogers, P.H. and Gardner, J.H., "Propagation of Sonic Booms in the Thermosphere", *J. Acoust. Soc. Am.*, Vol. 67, No. 1, pp. 78-91, 1980.

31. Maglieri, D.J., Carlson, H.W. and Hubbard, H.H., "Status of Knowledge of Sonic Booms", *Noise Cont. Eng.*, Vol. 15, No. 2, pp. 57-64, 1980.

32. Lomax, H., "The Wave Drag of Arbitrary Configurations in Linearized Flow as Determined by Areas and Forces in Oblique Planes", *NACA RM* A55A18, 1955.

33. Webster, A.G., *Partial Differential Equations of Mathematical Physics*, pp. 266-274, Dover Publications, INC. 1966.

34. Von Karman, Th. and Burgers, J.M., *Aerodynamic Theory*, W.F. Durand ed., Vol. 2, Springer, pp. 172-175, 1934.

35. Sears, W.R., "On Projectiles of Minimum Wave Drag", *Quart. Appl. Math.*, Vol. 4, No. 4, pp. 361-366, 1947.

36. Haack, W., " Geschossformen kleinsten Wellenwiderstandes", *Lilienthal-Gesellschaft für Luftfahrt*, Bericht 139, pp. 14-28, 1941.

37. Borsky, P.N., "Community Reactions to the Sonic Boom in the Oklahoma City Area", Aerospace Medical Research Laboratory Report AMRL TR-65-196, 1965.

38. Nixon, C.W. and Borsky, P.N., "Effects of Sonic Boom on People: St. Louis, Missouri, 1961-1962", Aerospace Medical Research Laboratory Report AMRL TR-65-37, 1965.

39. Kryter, K., et al., "Psychological Experiments on Sonic Booms Conducted at Edwards Air Force Base", Final Report, National Sonic Boom Office, Arlington Virginia, 1968.

40. Van der Velden, A. and Kroo, I., "Sonic Boom of the Oblique Flying Wing", *J. Aircraft*, Vol. 31, No. 1, pp. 19-25, 1994.

41. Carlson, H., "Correlation of Sonic-Boom Theory with Wind-Tunnel and Flight Measurements", *NASA TR* R-213, Dec. 1964.

42. Whitham, G.B., "The Flow Pattern of a Supersonic Projectile", *Comm. Pure Appl. Math.*, Vol. 5, pp. 301-348, 1952.

43. Ryshov, O.S. and Shefter, G.M., "On the Energy of Shock Waves Propagating in Moving Media", *Appl. Math. and Mech. (PMM)*, pp. 1293-1309, 1962.

44. Seebass, R. and George, A.R., "Sonic Boom Minimization", *J. Acoust. Soc. Am.*, Vol. 51, No. 2 (Part 3), pp. 686-694, 1972.